

Peak Criterion for Kernel Bandwidth Selection for Support Vector Data Description

Deovrat Kakde*, Arin Chaudhuri†, Seunghyun Kong‡, Maria Jahja§, Hansi Jiang¶, Jorge Silva||
and Anya Mcguirk¶,

Advanced Analytics Divison, SAS Institute
Cary, NC, USA

Email: *Dev.Kakde@sas.com, †Arin.Chaudhuri@sas.com, ‡Seunghyun.Kong@sas.com,
§Maria.Jahja@sas.com, ¶Hansi.Jiang@sas.com, ||Jorge.Silva@sas.com, **Anya.Mcguirk@sas.com,

Abstract—Support Vector Data Description (SVDD) is a machine-learning technique used for single class classification and outlier detection. SVDD formulation with kernel function provides a flexible boundary around data. The value of kernel function parameters affects the nature of the data boundary. For example, it is observed that with a Gaussian kernel, as the value of kernel bandwidth is lowered, the data boundary changes from spherical to wiggly. The spherical data boundary leads to underfitting, and an extremely wiggly data boundary leads to overfitting. In this paper, we propose an empirical criterion to obtain good values of the Gaussian kernel bandwidth parameter. This criterion provides a smooth boundary that captures the essential geometric features of the data.

I. INTRODUCTION

Support Vector Data Description (SVDD) is a machine learning technique used for single-class classification and outlier detection. SVDD is similar to Support Vector Machines and was first introduced by Tax and Duin [11]. It can be used to build a flexible boundary around single-class data. The data boundary is characterized by observations designated as support vectors. SVDD is used in domains where the majority of data belongs to a single class. Several researchers

have proposed use of SVDD for multivariate process control [1], [10]. Other applications of SVDD involve machine condition monitoring [12], [14] and image classification [8].

A. Mathematical Formulation

Normal Data Description:

The SVDD model for normal data description builds a minimum radius hypersphere around the data.

Primal Form:

Objective Function:

$$\min R^2 + C \sum_{i=1}^n \xi_i, \quad (1)$$

subject to:

$$\|x_i - a\|^2 \leq R^2 + \xi_i, \forall i = 1, \dots, n, \quad (2)$$

$$\xi_i \geq 0, \forall i = 1, \dots, n. \quad (3)$$

where:

$x_i \in \mathbb{R}^m, i = 1, \dots, n$ represents the training data,

R : radius, represents the decision variable,

ξ_i : is the slack for each variable,

a : is the center, a decision variable,

$C = \frac{1}{nf}$: is the penalty constant that controls the

trade-off between the volume and the errors, and, f : is the expected outlier fraction.

Dual Form:

The dual formulation is obtained using the Lagrange multipliers.

Objective Function:

$$\max \sum_{i=1}^n \alpha_i (x_i \cdot x_i) - \sum_{i,j} \alpha_i \alpha_j (x_i \cdot x_j), \quad (4)$$

subject to:

$$\sum_{i=1}^n \alpha_i = 1, \quad (5)$$

$$0 \leq \alpha_i \leq C, \forall i = 1, \dots, n. \quad (6)$$

where:

$\alpha_i \in \mathbb{R}$: are the Lagrange constants,

$C = \frac{1}{nf}$: is the penalty constant.

Duality Information:

Depending upon the position of the observation, the following results hold good:

Center Position:

$$\sum_{i=1}^n \alpha_i x_i = a. \quad (7)$$

Inside Position:

$$\|x_i - a\| < R \rightarrow \alpha_i = 0. \quad (8)$$

Boundary Position:

$$\|x_i - a\| = R \rightarrow 0 < \alpha_i < C. \quad (9)$$

Outside Position:

$$\|x_i - a\| > R \rightarrow \alpha_i = C. \quad (10)$$

The radius of the hypersphere is calculated as follows:

$$R^2 = (x_k \cdot x_k) - 2 \sum_i \alpha_i (x_i \cdot x_k) + \sum_{i,j} \alpha_i \alpha_j (x_i \cdot x_j). \quad (11)$$

$\forall x_k \in SV_{<C}$, where $SV_{<C}$ is the set of support vectors that have $\alpha_k < C$.

Scoring:

For each observation z in the scoring data set, the distance $\text{dist}^2(z)$ is calculated as follows:

$$\text{dist}^2(z) = (z \cdot z) - 2 \sum_i \alpha_i (x_i \cdot z) + \sum_{i,j} \alpha_i \alpha_j (x_i \cdot x_j). \quad (12)$$

The scoring data set points with $\text{dist}^2(z) > R^2$ are designated as outliers.

The circular data boundary can include a significant amount of space with a very sparse distribution of training observations. Scoring with this model can lead to many outliers being classified as in-liers. Hence, instead of a circular shape, a compact bounded outline around the data is often desired. Such an outline should approximate the shape of the single-class training data. This is possible with the use of kernel functions.

Flexible Data Description:

The Support Vector Data Description is made flexible by replacing the inner product $(x_i \cdot x_j)$ with a suitable kernel function $K(x_i, x_j)$. The Gaussian kernel function used in this paper is defined as:

$$K(x_i, x_j) = \exp \frac{-\|x_i - x_j\|^2}{2s^2} \quad (13)$$

where s is the Gaussian bandwidth parameter.

The modified mathematical formulation of SVDD with kernel function is as follows:

Objective function:

$$\max \sum_{i=1}^n \alpha_i K(x_i, x_i) - \sum_{i,j} \alpha_i \alpha_j K(x_i, x_j), \quad (14)$$

subject to:

$$\sum_{i=1}^n \alpha_i = 1, \quad (15)$$

$$0 \leq \alpha_i \leq C, \forall i = 1, \dots, n. \quad (16)$$

The results (7) through (10) hold good when the kernel function is used in the mathematical formulation.

The threshold R^2 is calculated as :

$$R^2 = K(x_k, x_k) - 2 \sum_i \alpha_i K(x_i, x_k) + \sum_{i,j} \alpha_i \alpha_j K(x_i, x_j) \quad (17)$$

$\forall x_k \in SV_{<C}$, where $SV_{<C}$ is the set of support vectors that have $\alpha_k < C$.

Scoring:

For each observation z in the scoring data set, the distance $\text{dist}^2(z)$ is calculated as follows:

$$\text{dist}^2(z) = K(z, z) - 2 \sum_i \alpha_i K(x_i, z) + \sum_{i,j} \alpha_i \alpha_j K(x_i, x_j). \quad (18)$$

The scoring data set points with $\text{dist}^2(z) > R^2$ are designated as outliers.

B. Importance of Kernel Bandwidth Value

The flexible data description is preferred when the data boundary is non-spherical. The tightness of the boundary is a function of the number of support vectors. In the case of a Gaussian kernel, it is observed that if the value of outlier fraction f is kept constant, the number of support vectors identified by the SVDD algorithm is a function of the Gaussian bandwidth parameter s . At very low values of s , the number of support vectors is high, approaching the number of observations. As the value of s increases, the number of support vectors reduces. It is also observed that at lower values of s , the data boundary is extremely wiggly. As s is increased, the data boundary becomes less wiggly, and it starts to follow the general shape of the data. At higher values of s , the data boundary becomes more spherical. The selection of an appropriate value of s is tricky and often involves experimentation with several values till a good data boundary is obtained. This paper provides an empirical criterion for selecting a good value of the Gaussian kernel bandwidth param-

eter. The corresponding data boundary is smooth and captures essential visual features of the data.

The rest of the paper is organized as follows. Section II illustrates how data boundary changes with s using two-variable data sets of known geometry. The empirical criterion for selecting a good value of s is introduced and validated. Section III provides analysis of real-life data using the proposed method. Section IV details a simulation study conducted to evaluate the proposed method on random polygons. A review of related work and comparison with existing methods are provided in Section V. Finally, conclusions and areas for further research are provided in Section VI.

II. PEAK CRITERION

We experimented with several two-dimensional data sets of known geometry to understand the relationship between data boundary and choice of bandwidth parameter. We considered the data boundary to be of good quality if it closely follows the contours of the data shape.

As one might guess, the value of the objective function (14) varies with the choice of bandwidth parameter, s . Denote this function: $V^*(s)$. Our experimentation revealed that the optimal s seemed to occur at the first critical point(s) of the first derivative of V^* with respect to s . In other words, the best s occurred where the second derivative of $V^*(s)$ equaled 0. In the remainder of this paper, we explore the usefulness of choosing s utilizing these findings. We refer to this method of selecting s as the Peak criterion. To examine the criterion's usefulness, we compute the first and second derivative values of $V^*(s)$ with respect to s using the method of finite differences and thus, do not make any statements about the existence of analytical derivatives.

To illustrate the approach and main findings of our experimentations, we focus on three data sets. These data sets adequately illustrate and capture our general

findings. The experimental approach and results are first explained in detail with a banana-shaped data set. We then follow with the results obtained from a star-shaped data set and a data set with three non-overlapping data clusters.

The two-dimensional banana-shaped data consists of 267 observations. The majority of the observations belong to a single class, with very few outliers (fraction outliers, $f=0.001$). Figure 2(a) provides a scatter plot of the data. To decide on a reasonable range of s to consider, we first examined how the number of support vectors varied with s (see figure 1). At low values of s , a majority of the 267 observations are identified as support vectors. As s increases, the number of support vectors generally decreases. For $s > 5$, the number of support vectors remains constant at 3. To cover all possible number of support vectors which can define the data boundary, we trained the data with the SVDD algorithm for s in the interval $[0.0001, 8.0]$, in increments of 0.05, keeping f constant at 0.001.

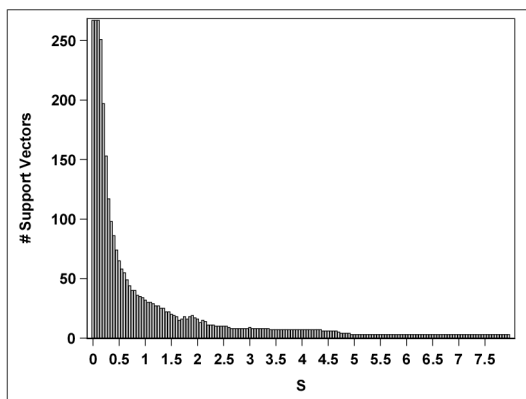


Fig. 1: Number of support vectors vs. s : banana-shaped data

At $s = 0.1$, each point in the data is identified as a support vector, representing a very wiggly boundary around the data. As the value of s increases from 0.1 to 0.35, the data boundary is still wiggly, with many “inside” points identified as the support vectors. A very well defined boundary around the data is first

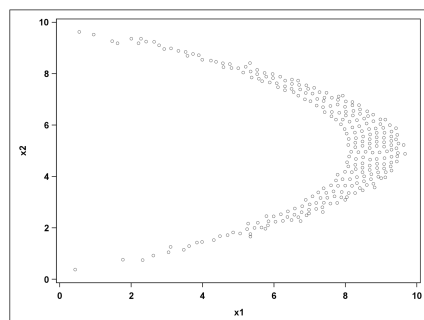
observed at $s=0.4$. As s increases from 0.4 to 1.1, the boundary continues to conform to the Banana shape, with the number of support vectors decreasing from 86 to 30. Beyond $s=1.1$, the number of support vectors decreases and the boundary starts losing its true banana shape. For $s \geq 4$, the support vectors envelope the outer parabola of the Banana shape. To confirm the shape of the data boundary, we score each training result on a 200×200 point data grid. Scoring results for select values of s are provided in Figure 2.

Figure 3 shows $V^*(s)$, the value of dual objective function (14) and its first derivative with respect to s , both plotted against s . $V^*(s)$ is a decreasing function of s . As s increases, the first derivative of $V^*(s)$ first decreases. Between $s=0.4$ to $s=1.1$, it remains relatively flat indicating the derivative has reached its first critical point and that the optimal s occurs here. After $s=0.8$, the first derivative starts to increase again.

Figure 4 shows the value of the second derivative of $V^*(s)$, with respect to s plotted against s . To decide if the value of the second derivative is zero, we fitted a penalized B-spline to the second derivative using the TRANSREG procedure available in the SAS software [9]. If the 95% confidence interval of the fitted value of second derivative contains zero, we consider the second derivative value to be approximately zero.

As seen in Figure 4, the second derivative is -0.20 at $s=0.20$. As s increases, the value of the second derivative starts increasing. Between $s=0.5$ and 0.85 , the second derivative is close to zero for the first time; we have the first set of first derivative critical points. All the values of s in this range provide a data boundary of good quality. The data boundary using $s=0.7$ is shown in figure 2(c). Compared to any other values of s outside the range $[0.4, 1.1]$, this data boundary captures the essential geometric properties of the banana-shaped data.

We performed similar experimentation using star-shaped data and a data set with three distinct data



(a) Scatterplot of banana-shaped data

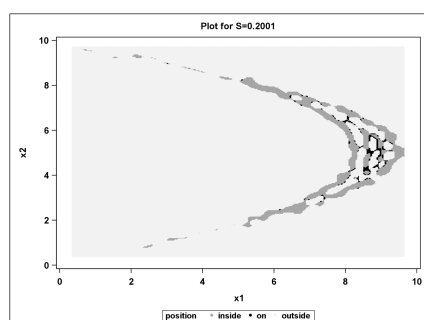
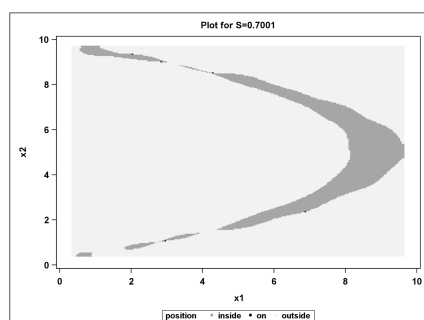
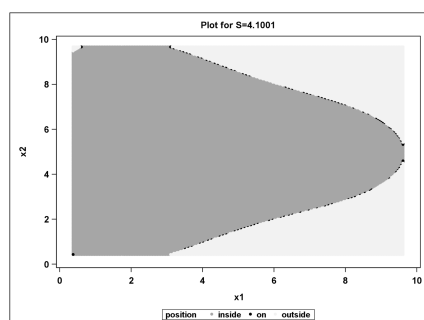
(b) $s=0.2$ (c) $s=0.7$ (d) $s=4.1$

Fig. 2: Data boundary for banana-shaped data. Fig (b) thru (d) show results of scoring on a 200x200 data grid. Light gray color indicates outside points, dark gray color indicates inside points and black color indicates support vectors.

August 10, 2017

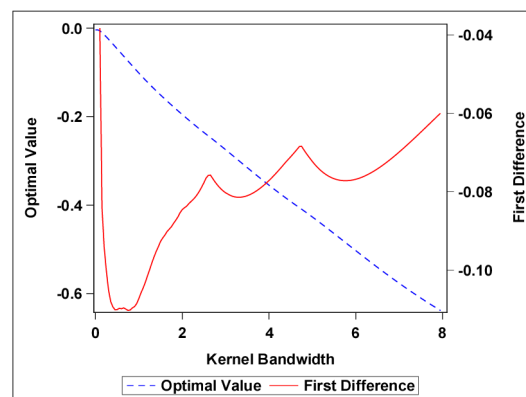


Fig. 3: Objective function value and first difference for banana-shaped data

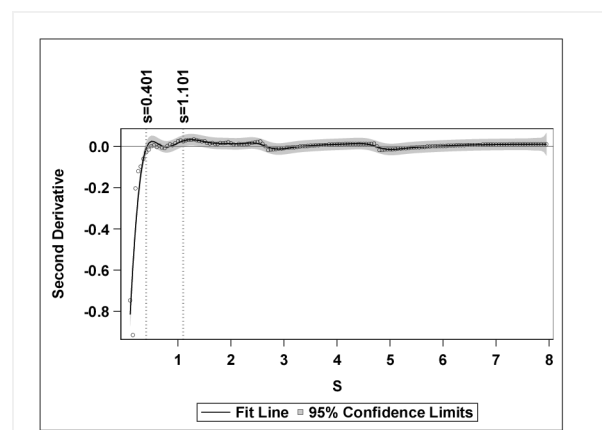


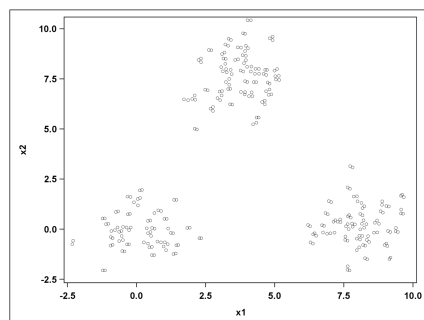
Fig. 4: Penalized B-spline fit for second derivative: banana-shaped data

clouds. The three cluster data was obtained from the *SAS/STAT User's guide* [9]. Figure 5(a) shows a scatter plot of this latter data set.

Similar to the banana-shaped data, we trained the three-cluster data set varying s from 0.001 to 8 in increments of 0.05. Scoring was performed on a 200x200 data point grid to confirm the shape of the data boundary. Scoring results for select values of s are provided in figure 5(b-d).

Figure 6 shows the second derivative of $V^*(s)$ with respect to s for the three-cluster data. The results are similar to the banana-shaped data. For s in $[1.0, 1, 25]$, the second derivative is close to zero indicating this is

DRAFT



(a) Scatterplot of three-cluster data

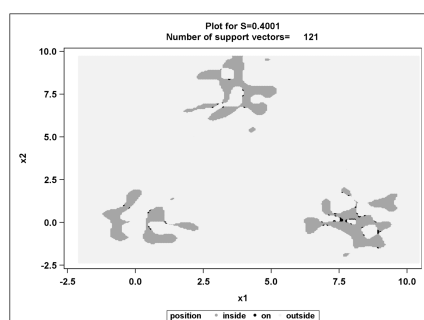
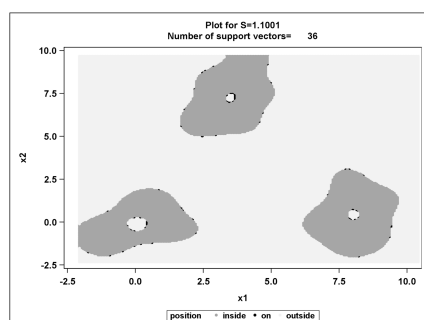
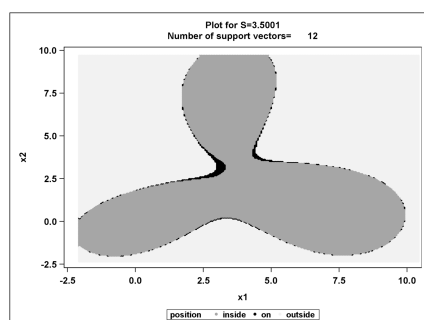
(b) $s=0.4$ (c) $s=1.1$ (d) $s=3.5$

Fig. 5: Data boundary for three-cluster data. Fig (b) thru (d) show results of scoring on a 200x200 data grid. Light gray color indicates outside points, dark gray color indicates inside points and black color indicates support vectors.

August 10, 2017

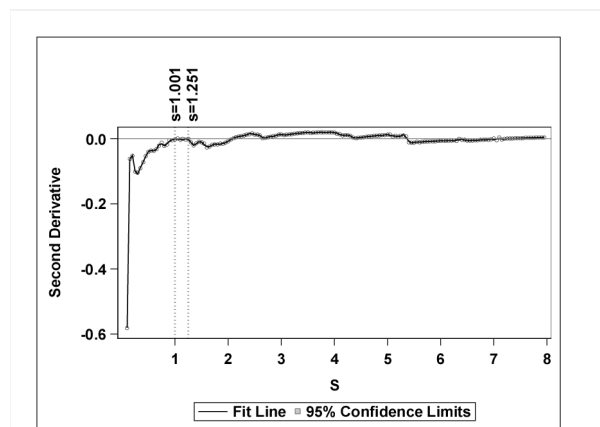
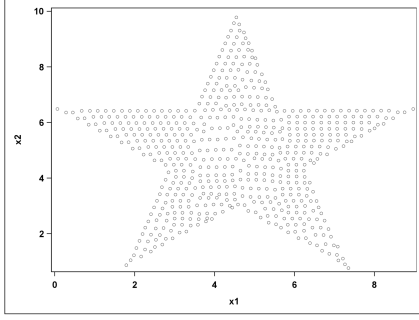


Fig. 6: Penalized B-spline fit for second derivative: Three-cluster data

the first set of critical points. For these values, high quality data boundaries were obtained. To illustrate, the data boundary using $s=1.1$ is shown in Figure 5(c). The boundary captures the essential geometric properties of the three-cluster data especially in comparison to any other values of s outside the first critical value interval (see Figure 6(b) and (d)). Next, we conducted our experiments with a star-shaped data set. Figure 7(a) shows the scatter plot of these data. This data set was trained using values of s from 0.001 to 8 in increments of 0.05. Scoring was performed on a 200x200 data point grid to confirm the shape of data boundary. Scoring results for select values of s are provided in Figure 7.

Figure 8 shows the second derivative of the optimal value of the objective function ($V^*(s)$) with respect to s for the star-shaped data. Between $s=0.75$ and $s=1.15$, for the first time, the second derivative is close to zero for the first time; the first, first derivative critical point is reached. A data boundary of good quality is observed at values of s between 0.75 and 1.15 (see Figure 7(c)); the data boundary captures the essential geometric properties of the data especially when compared to any other values of s (for examples, see Figure 7(b) and (d)).

DRAFT



(a) Scatterplot of star-shaped data

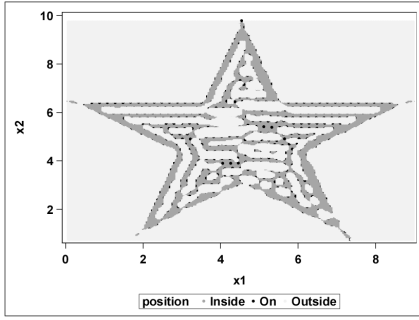
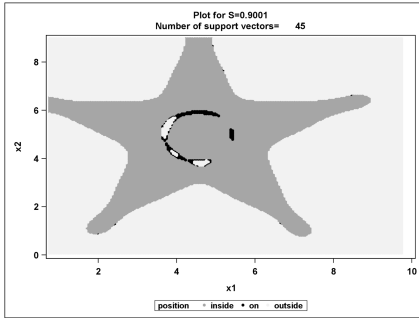
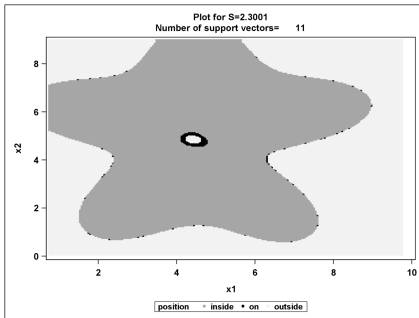
(b) $s=0.2$ (c) $s=0.9$ (d) $s=2.3$

Fig. 7: Data boundary for star-shaped data. Fig (b) thru (d) show results of scoring on a 200x200 data grid. Light gray color indicates outside points, dark gray color indicates inside points and black color indicates support vectors.

August 10, 2017

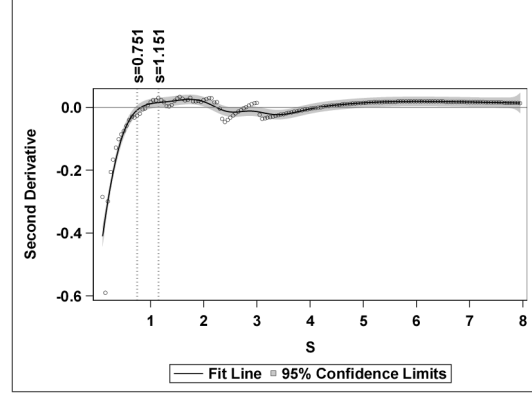


Fig. 8: Penalized B-spline fit for second derivative: star-shaped data

We tried our analysis on data sets with diverse geometrical shapes. For all data sets, the fact that a good quality data boundary can be obtained using value of s from the first set of critical points of the first derivative of $V^*(s)$, provides the empirical basis for our method.

III. ANALYSIS OF HIGH DIMENSIONAL DATA

Section II illustrated the value of using the Peak criterion to select s for different two-dimensional data sets. For such data sets a good value of s could be visually judged. Next, we want to test the criterion on higher dimensional data sets, where visual feedback about a good value of s is not possible. Instead, we see how the Peak criterion s values fare based on a measure used to assess model quality when labeled data are available. This criterion, known as the F_1 -measure [15] is defined as follows:

$$F_1 = \frac{2 \times \text{Precision} \times \text{Recall}}{\text{Precision} + \text{Recall}}, \quad (19)$$

where:

$$\text{Precision} = \frac{\text{true positives}}{\text{true positives} + \text{false positives}} \quad (20)$$

$$\text{Recall} = \frac{\text{true positives}}{\text{true positives} + \text{false negatives}}. \quad (21)$$

We chose the F_1 -measure because it is a composite measure that takes into account both Precision and

Recall. Models with higher values of the F_1 -measure are assumed to provide a better fit.

A. Analysis of Shuttle Data

The first higher dimensional data set we analyze is the Statlog (shuttle) data [6]. It consists of nine numeric attributes and one class attribute. Out of 58,000 total observations, 80% of the observations belong to class one. A random sample of 2000 observations belonging to class one, was selected for training. Scoring was performed to determine if the model could accurately classify an observation as belonging to class one. The SVDD model was trained and subsequently scored for values of s ranging from 1 to 100 in increments of 1. For each value of s the model performance was quantified using the F_1 -measure.

The plot of the F_1 -measure versus s is shown in Figure 9. A maximum value of F_1 -measure is obtained at $s=17$. Interestingly, the function is quite flat around $s=17$. In fact, the F_1 -measure is very similar for s in [15,20]. Figure 10 shows the plot of the second derivative of optimal value of objective function with respect to s plotted against s for this data. The values of s between 14 and 18, where the second derivative is nearly zero represents the first set of critical points. The fact that value of $s=17$ obtained using the F_1 -measure belongs to the set [14,18], obtained by the Peak criterion, provides the empirical evidence that Peak criterion works successfully with higher dimensional data.

B. Analysis of Tennessee Eastman (TE) Data

In this section we provide results of our experiments with the higher dimensional Tennessee Eastman data. The data were generated using MATLAB simulation code [7] which provides a model of an industrial chemical process [2]. The data were generated for

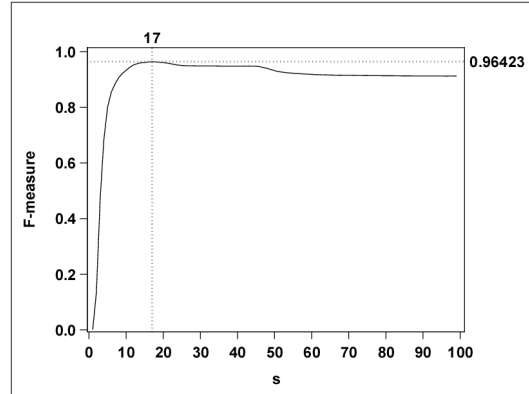


Fig. 9: Bandwidth parameter vs. F_1 measure: shuttle data

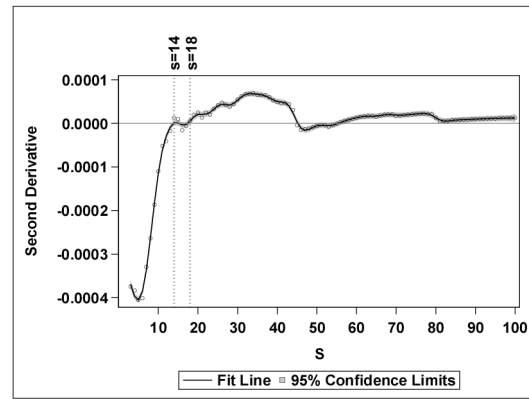


Fig. 10: Penalized B-spline fit for second derivative: shuttle data

normal operations of the process and twenty faulty processes. Each observation consists of 41 variables out of which 22 are measured continuously, on an average of every 6 seconds, and the remaining 19 are sampled at a specified interval either every 0.1 or 0.25 hours. We created our analysis data set using the simulated normal operations data for the first 90 minutes, followed by data corresponding to faults 1 through 20. A random sample of 200 observations belonging to normal operations, was selected for training. Scoring was performed on the remaining observations to determine if the model could accurately classify an observation as belonging to normal operations of

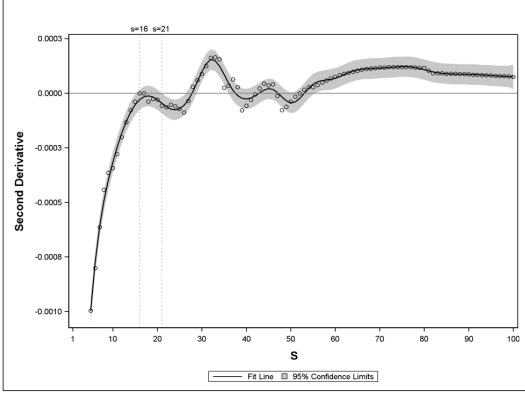


Fig. 11: Penalized B-spline fit for second derivative: Tennessee Eastman data

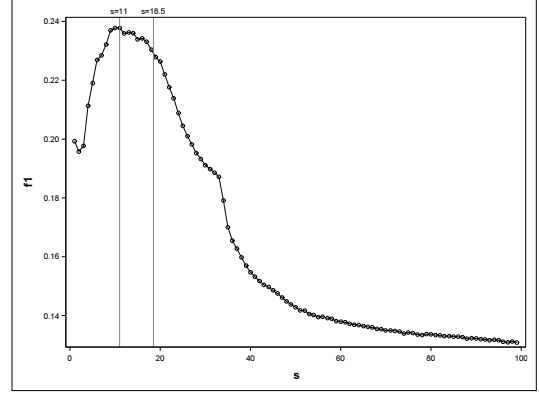


Fig. 12: Bandwidth parameter vs. F_1 measure: Tennessee Eastman data

the process. The SVDD model was trained and subsequently scored for values of s ranging from 1 to 100 in increments of 1. For each value of s the model performance was quantified using the F_1 -measure.

Figure 11 shows the plot of the second derivative of $V^*(s)$ with respect to s plotted versus s . The values of s between 16 and 21, where the second derivative is nearly zero, represent the first set of critical points. The plot of the F_1 -measure versus s is shown in Figure 12. A maximum value of F_1 -measure (0.2378) is obtained at $s=11$. The value of F_1 -measure at the midpoint of the s range suggested by the Peak criteria is 0.2291. The fact that the F_1 -measure value for the s value suggested by the Peak criteria is about 95% of the maximum value of the F_1 -measure, provides more empirical evidence that Peak criterion works successfully with higher dimensional data.

IV. SIMULATION STUDY

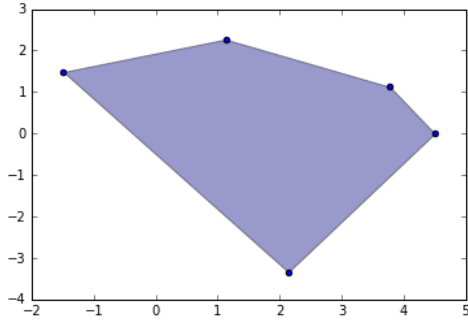
In this section we measure the performance of Peak criterion when it is applied to randomly generated polygons. Given the number of vertices, k , we generate the vertices of a randomly generated polygon in the anticlockwise sense as $r_1 \exp i\theta_{(1)}, \dots, r_k \exp i\theta_{(k)}$. Here $\theta_{(1)} = 0$ and $\theta_{(i)}$'s for $i = 2, \dots, n$ are the order statistics of an i.i.d sample uniformly drawn from

$(0, 2\pi)$. The r_i 's are uniformly drawn from an interval $[r_{\min}, r_{\max}]$.

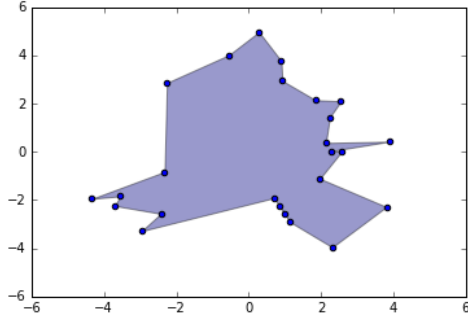
For this simulation we chose $r_{\min} = 3$ and $r_{\max} = 5$ and varied the number of vertices from 5 to 30. We generated 20 random polygons for each vertex size. Having determined a polygon we randomly sampled 600 points uniformly from the interior of the polygon and used this sample to determine a bandwidth using the Peak criterion. Figure 13 shows two random polygons.

However since we can easily determine if a point lies in the interior of a polygon we can also use cross-validation to determine a good bandwidth value. To do so, we found the bounding rectangle of each of the polygons and divided it into a 200×200 grid. We then labeled each point on this grid as an ‘‘inside’’ or an ‘‘outside’’ point. We then fit SVDD on the sampled data and scored the points on this grid for different values of s and choose that value that value of s that maximized the F_1 -measure.

The performance of the Peak criterion can be measured by the F_1 -measure ratio defined as $F_{\text{peak}}/F_{\text{best}}$ where F_{peak} is the F_1 -measure obtained when the value suggested by the Peak method is used, and F_{best} is the best possible value of F_1 -measure over all values of s .



(a) Number of Vertices = 5

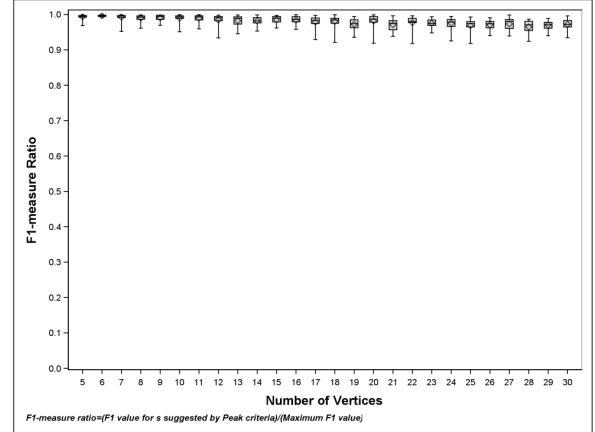


(b) Number of Vertices = 25

Fig. 13: Random Polygons

A value close to 1 will indicate that Peak criterion is competitive with cross-validation. We have 20 values of this ratio for each vertex size.

The Box-whisker plot in Figure 14 summarizes the simulation study results. The x-axis shows the number of vertices of the polygon and y-axis shows the F_1 -measure ratio. The bottom and the top of the box shows the first and the third quartile values. The ends of the whiskers represent the minimum and the maximum value of the F_1 -measure ratio. The diamond shape indicates the mean value and the horizontal line in the box indicates the second quartile. The plot shows that F_1 -measure ratio is greater than 0.9 across all values of number of vertices. The F_1 measure ratio in the top three quartiles is greater than 0.95 across all values of the number of vertices. As the complexity of the polygon increases with increase in number of vertices, we observed that the spread of F_1 -measure ratio also increased. The fact that F_1 -measure ratio is

**Fig. 14:** Box-whisker plot: Number of vertices vs. F_1 measure ratio

always close to 1, provides necessary evidence that the Peak criterion generalizes across different training data sets.

V. RELATED WORK

In support vector machines, cross-validation is a widely used technique for selecting the Gaussian bandwidth parameter [4]. Cross-validation requires training data that belongs to multiple classes. Hence, unless a good sample for normal class and outlier class is available, cross-validation is not a feasible technique for selecting Gaussian bandwidth parameter value in SVDD.

The Peak criterion is an unsupervised method that works on single class data. In this section, performance of the Peak criterion is compared against unsupervised methods for selecting Gaussian bandwidth parameter value published in the literature.

Method of Coefficient of Variation (CV) [3]:

Selects a value of s that maximizes the coefficient of variation of the kernel matrix.

$$CV = \frac{\text{Var}}{\text{Mean} + \epsilon} \quad (22)$$

where:

Var and Mean are variance and mean of the non-diagonal entries of the kernel matrix,

ϵ is a small value to protect against division by zero or round-off error. In our CV method computations, we set the value of ϵ to 0.000001.

Method of Maximum Distance (MD) [5]:

Obtains a value of s based on maximum distance between any pair of points in the training data.

$$s = \frac{d_{max}}{\sqrt{-\ln(\delta)}} \quad (23)$$

where:

$d_{max} = \max\|x_i - x_j\|^2$: maximum distance between any two pairs of points,

$$\delta = \frac{1}{n(1-f)+1},$$

n : Number of observation in training data,

f : the expected outlier fraction. In our MD method computations, we set the value of f to 0.001

Method of Distance to the Farthest Neighbor (DFN) [13]:

Uses distances of the training data points to their farthest neighbors and distances to their nearest neighbors. The optimal value of s is obtained by maximizing the following objective function:

$$f_0(s) = \frac{2}{n} \sum_{i=1}^n \max_{j \neq i} k(x_i, x_j) - \frac{2}{n} \sum_{i=1}^n \min_j k(x_i, x_j). \quad (24)$$

where:

n : number of observations in training data,

$k(x_i, x_j)$: kernel distance between observations i and j .

We calculated the values of s for the banana-shaped, three-cluster, and star-shaped data using the CV, MD and DFN method. Table I summarizes these results and also provides the value of s obtained using the Peak criteria.

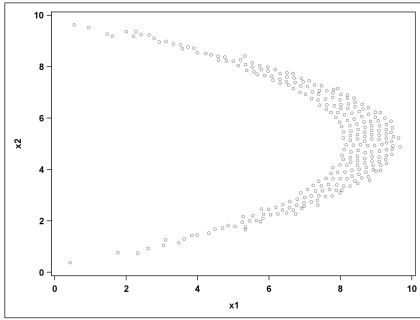
The scoring results using values of s recommended by above methods are illustrated in Figure 15, Figure 16 and Figure 17. For all three data sets, when compared against existing methods, the Peak criterion clearly provides a data boundary of best quality. The method of Coefficient of Variation also provides a data boundary of fairly good quality.

| Data | CV | MD | DFN | Peak |
|---------------|------|----|------|--------------|
| Banana | 0.5 | 46 | 1.99 | 0.4 to 1.1 |
| Three-cluster | 0.55 | 77 | 1.98 | 1.0 to 1.25 |
| Star | 0.48 | 35 | 1.98 | 0.75 to 1.15 |

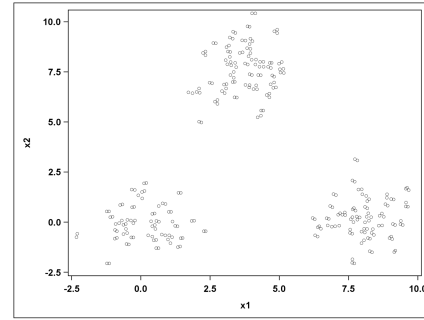
TABLE I: Comparison of s value

VI. CONCLUSIONS

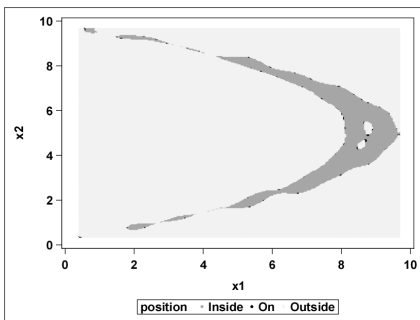
A criterion for selecting the value of Gaussian kernel bandwidth parameter s is proposed in this paper. Good quality data boundary that closely follows data shape can be obtained at values of s where the second derivative of optimal dual objective function value with respect to s first reaches zero. For certain data sets, the method provides a range of values where this criterion holds good. Any value of s within this range provides a good data boundary. Starting with a very low value of s , the search for a good value of s can be abandoned once the second derivative of the optimal objective function reaches zero. As outlined in Section V, the proposed method provides better results compared to existing methods. The criterion also provides good results when used for high dimensional data.



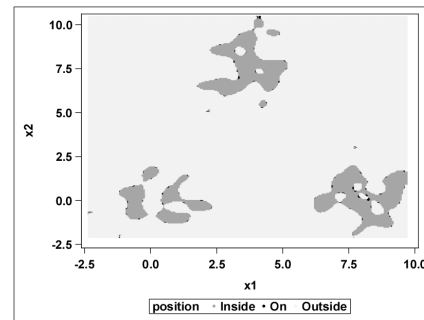
(a) Original data



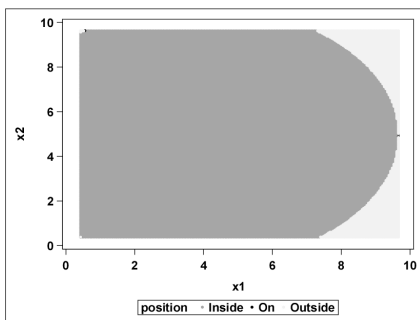
(a) Original data



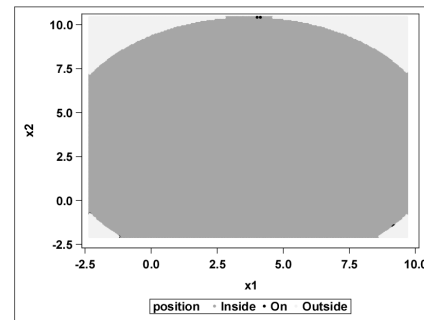
(b) CV



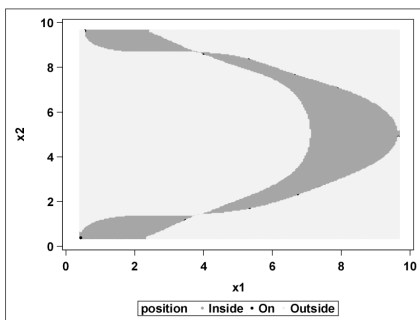
(b) CV



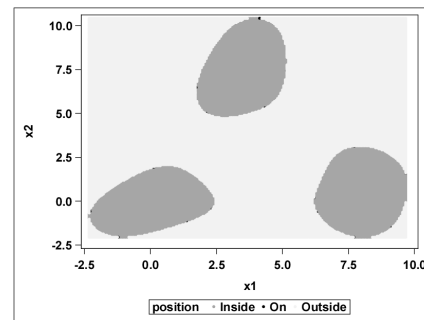
(c) MD



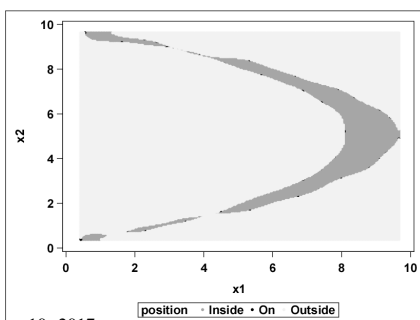
(c) MD



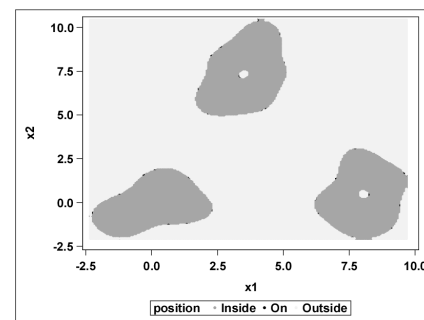
(d) DFN



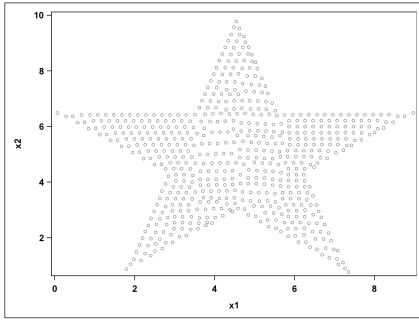
(d) DFN



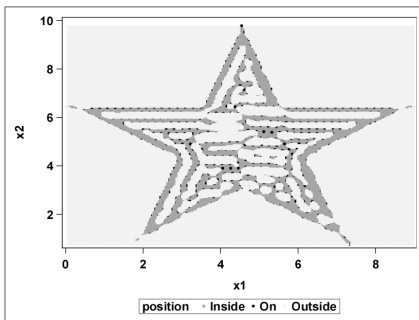
(e) Peak



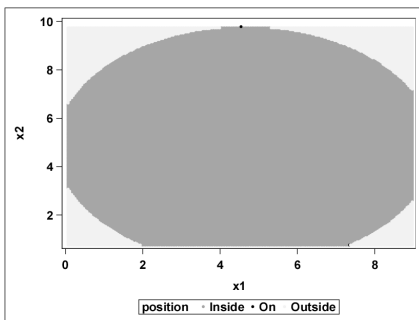
(e) Peak



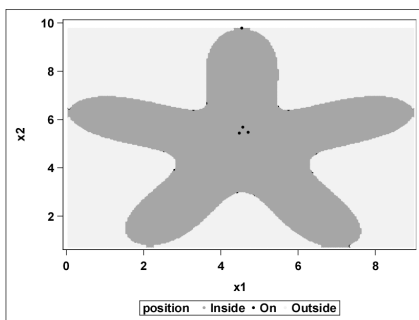
(a) Original data



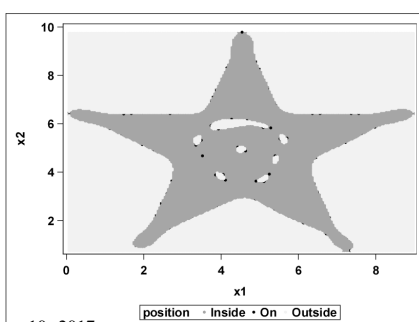
(b) CV



(c) MD



(d) DFN



(e) Peak

REFERENCES

- [1] Fatih Camci and Ratna Babu Chinnam. General support vector representation machine for one-class classification of non-stationary classes. *Pattern Recognition*, 41(10):3021–3034, 2008.
- [2] James J Downs and Ernest F Vogel. A plant-wide industrial process control problem. *Computers & chemical engineering*, 17(3):245–255, 1993.
- [3] Paul F Evangelista, Mark J Embrechts, and Boleslaw K Szymanski. Some properties of the gaussian kernel for one class learning. In *Artificial Neural Networks–ICANN 2007*, pages 269–278. Springer, 2007.
- [4] Trevor Hastie, Robert Tibshirani, and Jerome Friedman. *Un-supervised learning*. Springer, 2009.
- [5] Safa Khazai, Saeid Homayouni, Abdolreza Safari, and Barat Mojaradi. Anomaly detection in hyperspectral images based on an adaptive support vector method. *Geoscience and Remote Sensing Letters, IEEE*, 8(4):646–650, 2011.
- [6] M. Lichman. UCI machine learning repository, 2013.
- [7] N. Lawrence Ricker. Tennessee eastman challenge archive, matlab 7.x code, 2002.
- [8] Carolina Sanchez-Hernandez, Doreen S Boyd, and Giles M Foody. One-class classification for mapping a specific land-cover class: Svdd classification of fenland. *Geoscience and Remote Sensing, IEEE Transactions on*, 45(4):1061–1073, 2007.
- [9] SAS Institute Inc. *SAS/STAT 14.1 user's guide*, 2015.
- [10] Thuntee Sukchotrat, Seoung Bum Kim, and Fugee Tsung. One-class classification-based control charts for multivariate process monitoring. *IIE transactions*, 42(2):107–120, 2009.
- [11] David MJ Tax and Robert PW Duin. Support vector data description. *Machine learning*, 54(1):45–66, 2004.
- [12] Achmad Widodo and Bo-Suk Yang. Support vector machine in machine condition monitoring and fault diagnosis. *Mechanical Systems and Signal Processing*, 21(6):2560–2574, 2007.
- [13] Yingchao Xiao, Huangang Wang, Lin Zhang, and Wenli Xu. Two methods of selecting gaussian kernel parameters for one-class svm and their application to fault detection. *Knowledge-Based Systems*, 59:75–84, 2014.
- [14] Alexander Ypma, David MJ Tax, and Robert PW Duin. Robust machine fault detection with independent component analysis and support vector data description. In *Neural Networks for Signal Processing IX, 1999. Proceedings of the 1999 IEEE Signal Processing Society Workshop.*, pages 67–76. IEEE, 1999.
- [15] Ling Zhuang and Honghua Dai. Parameter optimization of kernel-based one-class classifier on imbalance learning. *Journal of Computers*, 1(7):32–40, 2006.